ARTICLE

Towards large area surface functionalization with luminescent and magnetic lanthanoid complexes

Received 00th January 20xx,
Accepted 00th January 20xx

DOI: 10.1039/x0xx00000x

Guillem Gabarró-Riera[a,b] Jesús Jover,[b,c] Juan Rubio Zuazo,[d,e] Elena Bartolomé,[f] E. Carolina Sañudo[a,b*]

Homogeneous surface deposition of molecules over a large area of substrate is difficult to achieve but extremely important for proposed applications of magnetic molecules in data storage, information processing or molecular spintronics. In this paper we report a simple method for large area surface functionalization with the aim of grafting complex molecules in an organized manner. Proof of concept is given grafting the complexes $[Ln_2(SYML)_3(H_2O)]$ (**1** Ln = Eu(III), **2** Ln = Dy(III)) on the functionalized Si(100) and using a combination of techniques, including luminescence to track the process. We obtain a homogenous coverage of Si(100) wafers (from 0.5 cm x 0.5 cm to 1 cm x 1 cm) with complexes **1** and **2**. Time of flight secondary ions mass spectroscopy (ToF-SIMS) confirms the presence of the expected molecular fragments on the surface. Grazing incidence X-Ray diffraction (GIXRD) measurements show preferred orientations and ordered domains of the molecules. The magnetic properties and anisotropy of the monolayer of grafted molecules are examined by X-Ray magnetic circular dichroism (XMCD), showing a fraction of molecules with a preferred orientation of their Easy Axis of Magnetization at 30° with respect to the surface-normal.

Introduction

As technology is constantly evolving, the fabrication of smaller and more efficient devices is an important goal. Over the last decades, single-molecule magnets (SMMs) have been proposed as building blocks for data storage devices, molecular spintronics applications or quantum information processing.[1] Although there is a vast number of studies published on this topic, the manipulation and addressing of single molecules on substrates is still a challenge to overcome to make possible these devices.[2] Simple magnetic molecules such as vanadyl phthalocyanine are shown to display two orientations on surfaces by high-resolution STM experiments.[3] In particular, large area coverage and a homogeneous orientation of molecules are two factors that are extremely important but at the same time difficult to achieve. The SMM properties and the influence of the environment in the latter (i.e. a quasicrystalline multilayer on a substrate or a submonolayer on a substrate) are key factors that must be addressed to achieve the proposed goals of using magnetic molecules on devices.

The first SMMs to be deposited on surfaces were the compound Mn_{12} and its numerous derivatives.[4,5] Since then, many different magnetic compounds have been deposited on different surfaces.[2,6–9] These studies show how the molecule-substrate interactions play a crucial role and how they are responsible of the loss of the interesting properties that these molecules had in bulk. For SMMs, a huge problem has been the lack of magnetization hysteresis while on a surface. In 2009 Sessoli reported the hysteresis of a tailor-made derivative of the family of Fe_4 SMMs on a Au(111) surface, showing that SMMs can be used to store information.[10] In 2016, giant hysteresis of $TbPc_2$ molecules on Ag(111) was observed when a thin layer of MgO was placed between the $TbPc_2$ molecules and the metallic substrate.[11] This result highlights the necessity of decoupling the magnetic molecule form the surface phonons and controlling the molecular orientation on the surface in order to preserve the molecular properties.

The organization of molecules on a 2-dimensional (2D) surface is thus a challenge. This can be done by using a long tether to graft the molecule, or by placing an intermediate layer between the substrate and the magnetic molecule. We have used dopamine[12] and oleic acid[12,13] on the surface of magnetic nanoparticles in order to decouple the magnetic properties of SMMs from the magnetic substrate. Synergy between magnetic molecular properties and substrate magnetism has been also observed with an intermediate layer[14] or without it,[15] in particular with highly anisotropic systems. The importance of phonons coupling to SMMs was shown in dysprociocenium SMMs[16,17] and record hysteresis temperatures have been achieved for these SMMs.[18,19]

[a.] *Institut de Nanociència i Nanotecnologia, Universitat de Barcelona (IN2UB), C/Martí i Franqués 1-11, 08028 Barcelona, Spain*
[b.] *Departament de Química Inorgànica i Orgànica, Secció de Química Inorgànica, C/Martí i Franqués 1-11, 08028, Barcelona, Spain*
[c.] *Institut de Química Teòrica i Computacional, Universitat de Barcelona (IQTC-UB). 08028, Barcelona, Spain*
[d.] *BM25-SpLine beamline at the ESRF, 71 Avenue des Martyrs, 38043, Grenoble, France*
[e.] *Instituto de Ciencia de Materiales de Madrid-CSIC, Sor Juana Inés de la Cruz, 3, Cantoblanco, 28049 Madrid, Spain*
[f.] *Escola Universitària Salesiana de Sarrià (EUSS), Passeig Sant Joan Bosco, 74, 08017 Barcelona, Spain*
[g.]

† Footnotes relating to the title and/or authors should appear here.
Electronic Supplementary Information (ESI) available: [details of any supplementary information available should be included here]. See DOI: 10.1039/x0xx00000x

In previous work in our group, we reported the synthesis and characterization of the compounds $[Yb_2(SYML)_3(H_2O)]$, $[Er_2(SYML)_3(H_2O)]$[20] and $[Dy_2(SYML)_3(H_2O)]$.[13] In this paper, we report the synthesis and characterization of $[Ln_2(SYML)_3(H_2O)]$ (**1** Ln = Eu(III)), a Eu analogue to the previously reported sandwich compounds. The complexes $[Ln_2(SYML)_3(H_2O)]$ (**1** Ln = Eu(III), **2** Ln = Dy(III)) are then deposited on functionalized Si(100) and the samples **1Si** and **2Si** are fully characterized. We obtain a large and homogenous coverage of Si(100) wafers of sizes between 0.5 cm x 0.5 cm to 1 cm x 1 cm with the complexes **1** and **2**.

Experimental section

All reagents are acquired from commercial sources and used as received. The ligand $SYMLH_2$ was prepared following the procedure reported by Gholizadeh *et al*.[20] The complex $[Dy_2(SYML)_3(H_2O)]$ (**2**) was prepared as reported.[13]

$[Eu_2(SYML)_3(H_2O)]$ (1)

The synthesis is adapted from the reported synthesis for the Dy (**2**),[13] Yb and Er analogues.[20] A stirred solution of SYML (0.1 g, 0.2 mmol), $Eu(NO_3)_3.5H_2O$ (0.064 g, 0.15 mmol) and Et_3N (100 µL, 0.6 mmol) in MeCN (20 mL) was heated under reflux for 2 h. After several days, orange crystals of complex **1** were obtained by slow evaporation. Yield: 54 %. IR (KBr, cm^{-1}): 1617(s), 1608(s), 1569(s), 1534(s), 1456(s), 1382(s), 1182(s), 982(w), 821(s), 726(s), 473(w). MS: $[Eu_2(SYML)_3(H_2O)]$ MW = 1565.3 g/mol. Ms/z ($M+1H^+-H_2O$) = 1548. Elemental Anal. Calc. for $[Eu_2(SYML)_3(H_2O)]\cdot H_2O$: C, 63.72; N, 5.31; H, 3.69. Experimental: C, 63.19; N, 5.41; H, 3.44.

Silanization of p-doped Si (Si-TSP)

Procedure modified from Godoy-Gallardo et al.[21]

Single side polished p-type Si(100) wafers were activated using a plasma arc-corona treater and immediately cleaned successively in an ultrasonic bath for two minutes in ethanol, 2-isopropanol, distilled water and acetone. The wafers were then dried with N_2 gas. Samples were introduced immediately into 8 ml of toluene and heated up to 80 ^oC under N_2 atmosphere. 16 µL of [(3-triethoxysilyl)propyl]succinic anhydride (TSP, >93%, TCI, ^1H NMR in ESI Figure S1) were added. After 15 minutes, functionalized Si wafers **Si-TSP** were cleaned in an ultrasonic bath in toluene for 5 minutes and dried with N_2. Samples were cured at 120 ^oC for 30 minutes in vacuum. Successive sample cleaning by sonication in ethanol, 2-isopropanol and acetone for two minutes was performed and the samples were finally dried with N_2. Resultant layer thickness was measured with ellipsometry and Atomic Force Microscopy (AFM). Hydrophobicity of the resultant surface was measured with a homemade contact angle (60^o).

Deposition of $[Ln_2(SYML)_3(H_2O)]$ on functionalized Si (1Si Ln = Eu(III), 2Si Ln = Dy(III))

Silanized **Si-TSP** samples were introduced in a vial with the reaction mixture of each compound and left for 2 minutes. Then, the wafers were removed from the solution and washed in clean MeCN, sonicated for 2 minutes and dried in a stream of N_2 gas. To avoid the presence of nanocrystals of the compound on the substrate, an additional cleaning with acetone in the ultrasonic bath (2 minutes) was performed.

Characterization techniques

Single crystal diffraction data for **1** were collected on a Bruker APEXII SMART diffractometer, using a microfocus Molybdenum Kα radiation source. The cif file is available free of charge form the Cambridge Structural Database (http://www.ccdc.cam.ac.uk/structures/2153928).

Luminescence was studied on a NanoLogTM-Horiba-Jobin Yvon iHR320 spectrophotometer using 280 nm excitation wavelength and the maximum opening of the slits (5 nm), on a solid sample holder oriented at 45^o to the incident beam and the front-face arrangement for the detector optics. Infrared spectra were collected in a FT-IR Thermo Scientific Nicolet™ iS5 Spectrometer equipped with an iD7 ATR accessory.

Elemental analyses were carried out at the *Serveis Cientificotècnics de la Universitat de Barcelona*, CCiTUB. Matrix Assisted Laser Desorption Ionization-Time of Flight (MALDI-ToF) mass spectroscopy experiments were performed at the *Unitat d'Espectrometria de Masses* at CCiTUB. Time-of-flight Secondary Ion Mass Spectroscopy (ToF-SIMS) measurements were performed at *Servicios de Análisis y Caracterización de Sólidos y Superficies de los Servicios de Apoyo a la Investigación de la Universidad de Extremadura* using a TOF-SIMS[5] from IONTOF GmbH (Germany), using Bi_3^{2+} ions with a primary gun energy of 25 KV. Spectra were collected by rastering the ion beam over a 300 µm x 300 µm sample area.

Contact angle measurements were carried out in a homemade instrument and analyzed with ImageJ plugin DropSnake.[22] Ellipsometry data were collected with a J.A. Woollam Alpha-SE ellipsometer and analyzed with CompleteEase software. AFM, SEM and XPS were performed at CCITUB. AFM images were collected with a Bruker MultiMode 8-HR with Nanoscope V controller electronics in ScanAssist mode in air. Nanoindentation experiments were made in contact mode. Scanning electron microscopy (SEM) images and energy dispersive X-ray spectroscopy (EDS) spectra were collected by a Jeol J-6510 scanning electron microscope equipped with an EDS and backscattered electron detector. X-ray photoelectron spectroscopy (XPS) data were collected with a PHI ESCA-5500 photoelectron spectroscope (X-ray source Al 1486.6 eV mono at 300.0 W). Cleaning of the samples was performed using ultrasound cleaning bath VWR USC600TH at room temperature. Simultaneous Hard X-ray Photoelectron Spectroscopy (HAXPES) and Grazing Incidence X-ray Diffraction (GIXRD) data were collected in ultra-high vacuum (P = $1x10^{-10}$ mbar UHV) conditions using a photon energy of 12 keV at the BM25-SpLine beamline at the European Synchrotron ESRF.[23] The diffraction data was collected using a massive S2D3 diffractometer equipped with a 2D detector, while the HAXPES data was obtained using a specially developed high kinetic energy analyzer HV-CSA300 able to work up to kinetic energies of 15 keV.[24]

Soft X-ray absorption spectroscopy (XAS) and X-ray magnetic circular dichroism (XMCD) experiments were performed at the BOREAS beamline of ALBA synchrotron radiation facility. All spectra were recorded using Total Electron Yield (TEY) detection mode, with a 90% circularly polarized light and fields up to 6 T. The nominal set temperature was 1.5 K, however, the fitting of the magnetization curves indicates that the real temperature in the samples was higher, 4 K. The **2Si-1** sample was glued with silver paint to a copper sample holder, placed perpendicular to the synchrotron ring plane (xy). The powdered sample of complex **2** was crushed onto an indium foil to ensure good thermal contact. The XMCD (μ^-- μ^+) and XAS (μ^-+ μ^+/2) spectra at the $M_{4,5}$ edge of Dy at 6 T were determined from four x-ray absorption spectra measured under right-handed (μ^+) and left-handed (μ^-) circular polarizations. To perform angle-dependent experiments the sample was rotated about a vertical axis (z), perpendicular to the synchrotron ring, so as to vary the angle of incidence between the X-ray beam and the substrate-normal (θ), between θ = 0º (normal incidence) and θ = 70º (grazing incidence). To avoid radiation damage, experiments were done at low flux. XMCD(*B*) cycles were performed by following the resonant M_5 peak while sweeping the magnetic field between 6 T and -6 T and back, at a rate of 2 T/min. The absolute XMCD(*B*) scale was fixed at *B* = 6 T to the total magnetization moment value obtained from a full energy range XMCD scan.

Results and discussion

Following our work on Schiff base lanthanoid sandwich complexes of general formula $[Ln_2(SYML)_3(H_2O)]$[13,20] we prepared an Eu analogue, with the objective to add the Eu luminescence to the multifunctional complexes. The goal was to use lanthanoid luminescence of the surface deposited molecules as an easy way to track the deposition process. The ligand used is a Schiff base shown in Figure 1a with flat aromatic naphtyl groups that has a tetradentate coordination pocket of 2 N and 2 O donors. The coordination pocket is too small for a lanthanoid and provides sandwich complexes with these ions. In our experience, only Cerium(IV) forms the mononuclear complex $[Ce(SYML)_2]$ and this is due to the possibility of attaining a +4 oxidations state for Cerium.[25] The synthesis of the complex followed the reported procedure for Yb(III), Er(III) and Dy(III), where the Ln(III) salt is added to MeCN solution of the ligand in the presence of a weak organic base to facilitate the deprotonation of the phenol groups of the SYML ligand. Orange crystals of a dinuclear Eu(III) complex of formula $[Eu_2(SYML)_3(H_2O)]$ (**1**) are obtained as expected in moderate yield. The crystal structure of **1** is shown in Figure 1b-e and the crystallographic and data collection parameters are listed in Table 1. Complex **1** is isostructural to the Dy analogue[13] (compound **2** in this paper) and to the Er and Yb analogues previously reported.[20]

Table 1. Crystallographic and data collection parameters for complex **1** at 100 K.

Crystal system	Triclinic	Space group	P-1
a/Å	10.589(6)	Formula	[Eu2(SYML)2(H2O)]·H2O
b/ Å	18.019(9)	T / K	100 K
c/ Å	18.633(10)	λ / Å	0.71073
α/°	67.421(12)	D/ g/cm3	1.663
β/°	74.502(17)	R1	0.0719
γ/°	87.982(10)	wR2	0.1844
Volume/ Å^3	3153(3)	Goodness of the fitting	0.962
Z	2	CCDC #	2153928

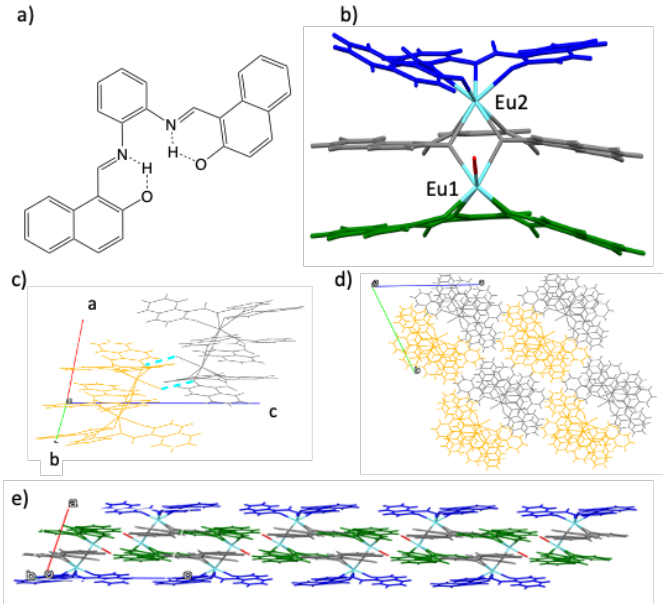

Fig. 1 (a) The ligand $SYMLH_2$. (b) Crystal structure of complex **1**, where each SYML ligand is shown in one colour, Eu in cyan and the coordinated water molecule in red. (c) Supramolecular dimer with H-bonds between the two molecules of 1 in the unit cell shown in grey and yellow, H-bonds shown as dashed cyan lines. (d) Crystal packing view along a-axis of the unit cell. (e) Crystal packing view along the bc plane of the unit cell

Complex **1** is a double-double-decker complex or a double sandwich. Each Eu(III) ion is sandwiched between two SYML ligands. The central Schiff base ligand (grey in Figure 1b) actively uses the two oxygen atoms to bridge the two lanthanoids. The coordination spheres of the two Eu(III) ions in the complex are not equal. Eu1 is in an O_5N_2 coordination pocket with two nitrogen and four oxygen atoms of SYML ligands and one coordinated water molecule (in red in Figures 1b and 1d). Eu2 in Figure 1b is located in a O_4N_4 coordination pocket of two completely deprotonated SYML ligands.

The two molecules of **1** in the unit cell (one in yellow and the other in grey) form a supramolecular dimer by establishing H-bonds between the coordinated water molecule on one molecule of **1** and one O-donor from a SYML ligand of the

neighboring molecule, shown in Figure 1c. Complex **1** stacks on columns along the a-axis of the unit cell, forming two columns. Each molecule in one column has 2 H-bonds with a partner in the next column forming the above described supramolecular dimer, and two H-bonds with the next molecule in the other column, mediated by the solvation H_2O. Along the bc plane of the unit cell, molecules form a closely packed layer, view along a in Figure 1d and side view in Figure 1e. The height of this layer is approximately 1 nm.

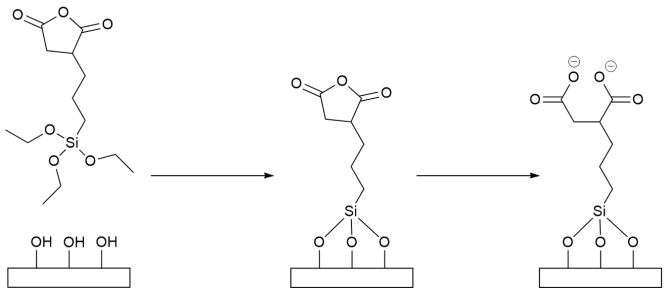

Fig. 2 Schematic representation of the functionalization procedure using TSP ((3-triethoxysilyl)propyl]succinic anhydride) and hydrolysis of the succinic anhydride to obtain exposed carboxylato groups.

We chose Eu (**1**) and Dy (**2**) complexes for surface deposition: Europium is luminescent, so the presence of the lanthanoid ion on the substrate can be followed using this technique and the Dy analogue is a known SMM. In a prior work we observed how an organic layer of oleic acid helped preserve the magnetic properties of **2** when physiosorbed on iron oxide nanoparticles with a monolayer of oleate.[13] The shape anisotropy of the molecules makes them good candidates for surface deposition.

Furthermore, these type of sandwich molecules are known with terminal carboxylato or nitrato groups, instead of one of the ligands.[20,26] Thus, one of the ligands of **1** could be exchanged by one or two carboxylato groups, and this could be exploited to perform on-surface chemistry to graft **1** on a suitably functionalized surface. The terminal carboxylato group should be part of a linker that is long enough to avoid strong coupling of the Ln_2 core to the surface.

The described procedures for the silanization of metal and metal oxides[21] can be applied to silicon wafers. In this work we have used Si(100) wafers. The reported procedure has been adapted to obtain a homogeneous coverage of (triethoxysilyl)propyl succinic anhydride (TSP).[21] In the presence of water the cyclic anhydride opens exposing two carboxylato groups, which then could substitute a SYML ligand and chemisorb the magnetic molecule on the substrate (Figure 2).

In order to start with a homogenous surface, we have activated the surface by an arc-corona treatment in air where a plasma is produced between an electrode and the silicon wafer. Upon activation the silicon wafer becomes extremely hydrophilic due to the high concentration of hydroxyl groups. The activation of the surface is monitored by checking the hydrophilicity of the surface by contact angle of a water droplet. Before silanization, the contact angle of the Si(100) with its native oxide is 56 ± 8 °. Once the surface is activated the water droplet completely wets the surface. The activated samples are introduced in a solution of TSP/toluene. With silane concentration of 0.2% and deposition time of 15 minutes silane layers of 1.40 ± 0.53 nm are obtained.

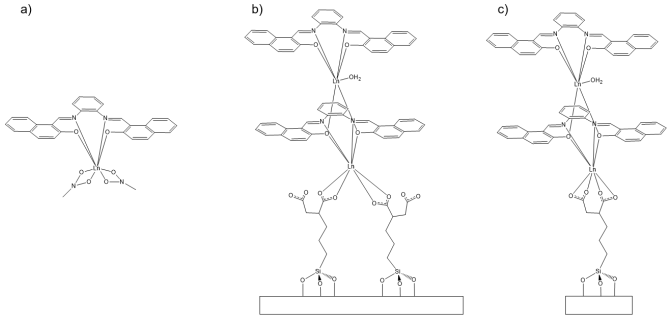

Fig. 3 (a) A $[Ln(SYML)(NO_3)_2]^-$ fragment. (b) and (c) Two possible anchoring modes of $[Ln_2(SYML)_3(H_2O)]$ to the Si-TSP substrate.

The **Si-TSP** wafers are characterized by contact angle, ellipsometry and SEM/AFM. The measured contact angle after silanization is 60°, indicating a slightly more hydrophobic substrate, which is expected for the **Si-TSP** samples. AFM showed homogeneous and complete coverages of the Si wafer of approx. 1 cm x 1 cm with an average roughness for **Si-TSP** of R_a = 0.287 ± 0.03 nm, (see ESI Figure S2).

The ensemble $[Ln(SYML)_2]^-$ is charged and thus neutral species of formula $[Ln_2(SYML)_3(H_2O)]$ crystallize easily. There are several examples in the literature of complexes with one lanthanoid sandwiched between one Schiff base ligand and two or more terminal ligands like the fragment shown in Figure 3a. This fragment contains one planar ligand and two or three chelates (nitrato, acetylacetonato, carboxylato or other tripodal ligands).[20,26,27] In our previous paper, we studied this reaction mixture in detail and learnt that it contains Ln+SYML aggregates that crystallize over 2-3 weeks to form complexes **1** or **2**.[20] Based on this and our insight on the reaction mixture components, we chose to use the reaction mixture to perform on-surface chemistry with the carboxylato groups exposed after hydrolysis of the succinic anhydride in **Si-TSP**. This procedure aims to covalently attach the $[Ln_2(SYML)_2]^{2+}$ (Ln = Eu, **1**; Dy, **2**) fragments onto the surface, as shown in Figures 3b and 3c. The O-N distance from one SYML ligand in **1** or **2** is 2.7 Å, while the typical O-O distance from a chelating carboxylato group is 2.2 Å. Thus, a coordination mode like the one shown in Figure 3b will cause only a small distortion of the coordination environment of the lanthanoid in **1** or **2**, while a coordination as the one shown in Figure 3c would most likely be too sterically hindered to occur.

The **Si-TSP** wafers are immersed in the reaction mixture of complexes **1** or **2**. Wafers with grafted **1** and **2** are called **1Si** and **2Si**. After a given time, the wafers are removed from the solution and cleaned in an ultrasound bath in acetonitrile and acetone, successively. Several samples are obtained, with layers of the compounds of different thicknesses, as summarized in Table 2.

Table 2. Characterization data for silanized **Si-TSP** wafers functionalized with **1** or **2, 1Si** and **2Si**. Each batch of wafers prepared under the same conditions are called **1Si-n** or **2Si-n**.

Sample	Ln	Contact angle (°)	Layer (nm)	Conditions
Si-TSP	--	60	1	0.2% v/v, 15 minutes
1Si-1	Eu	80	1	10 minutes + acetone cleaning
1Si-2	Eu	80	1 + nanocrystals	10 minutes. No acetone cleaning
1Si-3	Eu	80	bulk	10 days deposition
2Si-1	Dy	73	1	10 minutes deposition + acetone cleaning
2Si-2	Dy	73	4	24h deposition. No acetone cleaning

Two key parameters were found to impact the substrate functionalization: (i) deposition time, and (ii) proper cleaning with a solvent in which **1** and **2** are soluble, e.g. acetone. As for deposition times, 10 minutes allowed to obtain reproducible thicknesses of around 1 nm. AFM images are shown in Figure 4. If the wafers are only rinsed with clean solvent instead of cleaned in the ultrasound bath, small nanocrystals are found on the surface (Figure 4a). These are successfully removed after ultrasound cleaning in acetone. (Figure 4b). After 24h of deposition, AFM shows a completely covered surface with a large number of bigger objects, the average roughness is Ra = 1.3 ± 0.19 nm (ESI Figure S3).

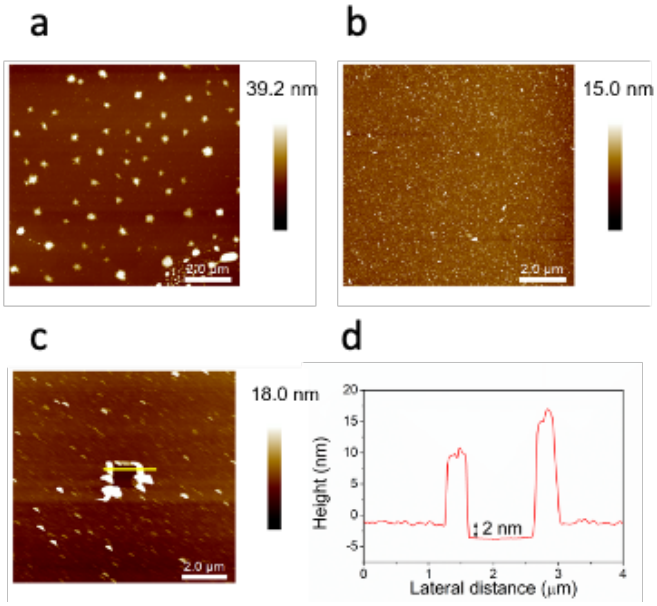

Fig. 4 (a) 10 µm x 10 µm AFM image of **1Si-2**, where star-shaped crystals of **1** are observed after 10 minutes deposition without acetone cleaning; (b) 10 µm x 10 µm AFM image of **1Si-1** after 10 minutes deposition with acetone cleaning. (c) Nanoindentation on **1Si-1** and (d) height profile.

The thickness of the obtained layers was checked by ellipsometry. This technique provides the average thickness of the area covered by the laser beam. If very long deposition times were used, such as several days, bulk-like layers of **1** that could be observed with the naked eye (**1Si-3**) were obtained (ESI material Figure S3). For this sample **1Si-3**, it was not possible to measure the thickness by ellipsometry due to the roughness of the layer of microcrystals of **1**. For the thin layers, ellipsometry provided values of 1 nm for **1Si-1** and **2Si-1**; these values are the expected for one monolayer of molecules or supramolecular dimers as those shown in Figure 1c.

AFM nanoindentation experiment confirmed the thicknesses measured by ellipsometry with very good agreement, Figure 4c and 4d shows an AFM image of a nanoindentation experiment on sample **1Si-1** with its corresponding height profile. In order to corroborate the homogeneity of the functionalization several AFM images at different spots on the **1Si-1** wafer were taken. All images were similar, with an average roughness, R_A, of 0.68±0.05 nm (see ESI material for the full series of images, Figure S4). The topographical information obtained by AFM is consistent with the goal of a homogeneous functionalization of the **Si-TSP** wafers.

To obtain compositional information of the layers, XPS spectra were collected for different samples of both **1Si** and **2Si**. Selected spectra are shown in Figure 5. In all cases we observed the expected peaks for Eu and Dy. These data do not confirm that on-surface chemistry has taken place, as a simple physiosorbed layer of compounds **1** and **2** would give similar response in XPS. However, the atomic percentage can be used to check the expected N/Ln ratio for each proposed system. For a layer of physiosorbed complexes **1** or **2**, the expected N/Ln ratio is 6/2 = 3 as obtained by XPS of the bulk compound. A layer of chemisorbed $[Ln_2(SYML)_2]^{2+}$ fragments should present a N/Ln ratio of 4/2 = 2. The XPS spectra of **1Si-1** are shown in Figure 5a. The calculated N/Eu ratio for **1Si-1** is 1.7, a value that is close to the expected for a layer of chemisorbed $[Ln_2(SYML)_2]^{2+}$ fragments. For thicker layers, this ratio increases, indicating the existence of a higher number of full molecules. For example, sample **2Si-2** shows by ellipsometry a compound layer of 4 nm with the observed experimental ratio of 3.06 (Figure 5).

The XPS X-ray beam only penetrates about 10 nanometers in the sample, so the intensity of the different Si2p peaks (~103.5 eV for SiO_2 and ~99 eV for elemental Si) is a direct proof of the deposited layer's thickness. As thicker layers are obtained, the intensity of the peak at 103.5 eV increases and the one at 99.4 eV decreases (ESI material, Figure S5), supporting the measurements made by ellipsometry and AFM nanoindentation.

Hard X-Ray Photoemission Spectroscopy (HAXPES) data were collected at beamline BM25 at the European Synchrotron ESRF. HAXPES allows us to check the composition of the monolayer deposited on **Si-TSP** and we were able to confirm the presence of europium and nitrogen in sample **1Si-1**. Figure 6 shows the HAXPES spectra for the N1s and Eu2p core levels. For N1s core level photoemission, a peak with a maximum at 401 eV is observed (Figure 6a). This value is shifted from the expected 409 eV for elemental nitrogen, and it agrees with a value of circa. 400 for C-NH_2. XPS spectra of bulk **1** and **2** present the N1s peak at 399 eV, which also agrees with the observed by HAXPES.

The Eu 2p1/2 peak shows two features at 1612 and 1620 eV. The expected peak for Eu 2p1/2 metal is 1617 eV.

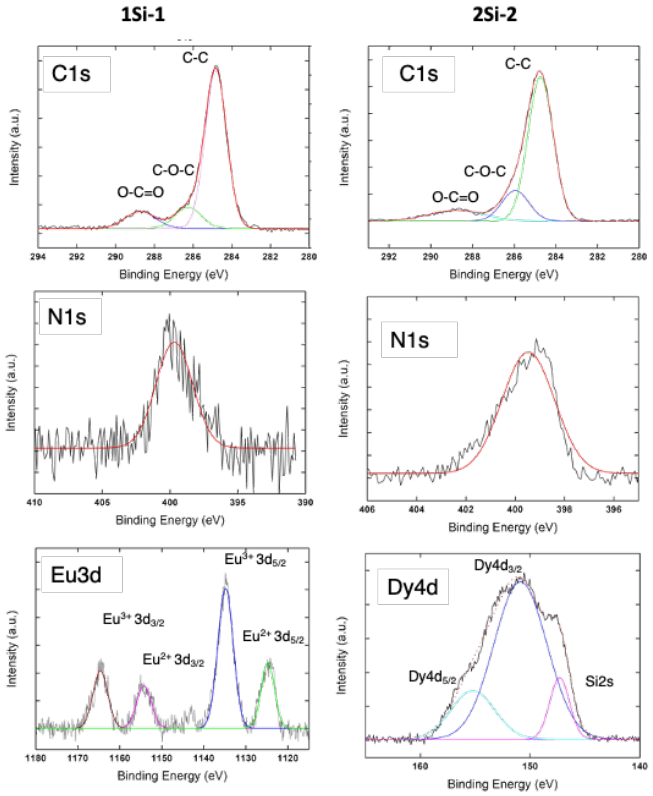

Fig. 5 Corrected XPS energy regions for C1s, N1s and Eu3d of **1Si-1** and C1s, N1s and Dy4d of **2Si-2**.

The observation of two peaks with a separation of 8 eV is consistent with Eu(III) reduction to Eu(II) on the surface grown layer of EuSYML.[28] Eu cations can be either in a divalent Eu2+ state with half-filled 4d10 4f7 shell or exist as trivalent Eu3+ with a 4d10 4f6 level, which is chemically shifted toward higher binding energies by reduced Coulomb repulsions. The peaks are too close for a good integration so we have used a simple maximum height ratio that shows an approximate ratio of 3:2 Eu3+ to Eu2+, the reduction to Eu2+ takes place in the UHV conditions of HAXPES by injection of electrons in the sample.

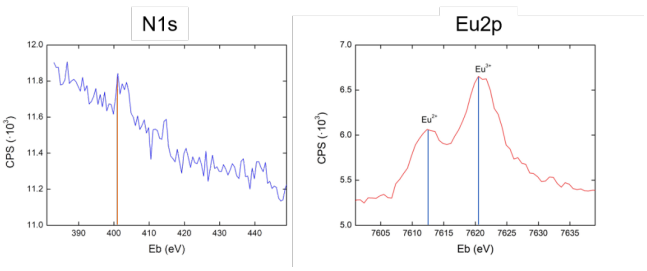

Fig. 6. HAXPES spectra for sample **1Si-1**, showing N1s and Eu2p peaks.

We previously reported these complexes fly well in mass spectroscopy so MALDI-ToF spectra from the reaction mixture and **1Si-1** and **2Si-1** silicon wafers were collected, (ESI Figure S6). For the reaction mixture, we observe two main peaks at 983 m/z and 1546 m/z for the Eu compound, and at 992 m/z and 1568 m/z for the Dy analogue. These peaks correspond to the monomer compound $[[Ln(SYML)_2] + H]^+$and the whole molecule without a water molecule $[[Ln_2(SYML)_3] + H]^+$. For **2Si-2** we could observe the expected peaks, confirming the presence of intact molecules on the surface (See ESI, Figure S7). For samples **1Si-1** and **2Si-1**, these peaks were not observable, probably due to the low amount of sample on the surface. For this reason, we performed a ToF-SIMS experiment, which is a surface-sensitive technique. In this case, an ion beam is used to remove all the material from the surface. The ion beam is more powerful than the laser used in MALDI, so no whole molecules could be observed. However, single ions Eu+ and Dy+ were observed distributed throughout a 300 µm x 300 µm, corroborating once more the homogeneity of our functionalization. It is worth mentioning that for **2Si-1,** we could observe the fragment of $[Dy(SYML)]^+$ at 578 m/z, which confirms the presence of the Ln-SYML compounds on the surface. In Figure 7c we can observe that this fragment is present homogeneously on the substrate. On the other hand, for the Eu analogue **1Si-1**, we did not observe this fragment. This can be due to the possible reduction to Eu(II), which would generate a neutral [Eu(SYML)] fragment.

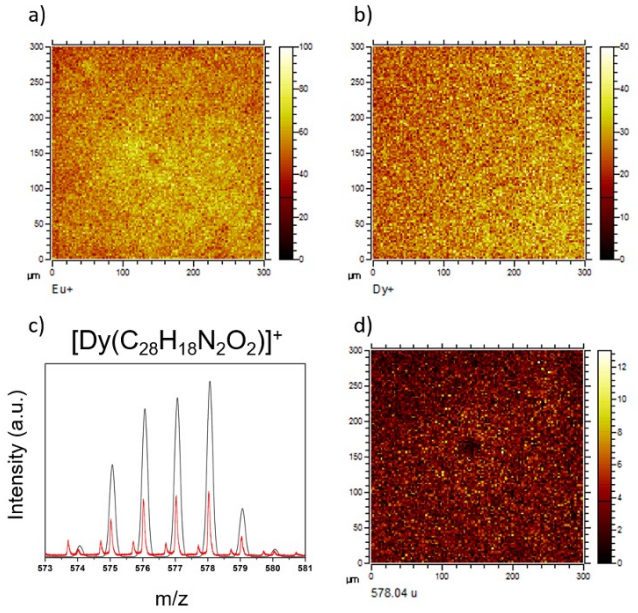

Fig. 7. (a) Distribution Eu^+ ions on **1Si-1**. (b) Distribution Dy^+ ions on **2Si-1**. (c) Experimental ToF-SIMS peak corresponding to $[Dy(SYML)]^+$ (578.04 m/z) in red, the calculated isotopic distribution is shown in black. (d) Spatial distribution of the $[Dy(SYML)]^+$ (578.04 m/z) peak on a 300 µm x 300 µm area of the substrate.

We want to use luminescence as a tool to ascertain the presence of the molecules on the surface, so we studied the emission spectra of the bulk solid **1** and compared it with the emission spectra of samples **1Si**. The characteristic emission of Eu(III) was observed, at an excitation wavelength of 280 nm (Figure 8). In solution, emission is dominated by the ligand

emission band, as already reported.[29] Upon excitation at 280 nm, the Eu(III) emission can be observed for the surface functionalized wafers **1Si-1**, **1Si-2** and **1Si-3**, as shown in Figure 8. This clearly shows that Eu(III) luminescence can be used to track surface functionalization with Eu(III) complexes. We believe this procedure can be extended to other strongly luminescent lanthanoids like Tb(III). The data on these **1Si** and **2Si** samples show that Ln(III) (Ln = Eu, Dy) and SYML ligands are present in the monolayer.

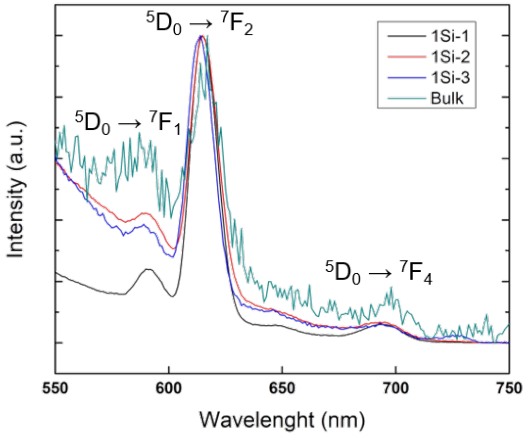

Fig. 8. Solid-state emission spectra of samples **1Si-1, 1Si-2** and **1Si-3** and powder **1** upon excitation at 280 nm. Intensities have been normalized to the $^5D_0$->$^7F_2$ peak.

The cartoon of Figure 9a is the simplest arrangement of the complexes on the surface for **1Si** and **2Si**. In this cartoon a layer of the height of the a-axis in the unit cell (shown in red) is grown on the substrate, following the same self-assembly of dimers of the **1** and **2** complexes along the bc plane, with either the blue or green ligand of alternating molecules in Figures 1b and 1d exchanged by the carboxylato groups of **Si-TSP**.

To confirm this model, GIXRD studies were performed at beamline BM25 at the European Synchrotron ESRF. The signal of thin layers is maximized by using a small incidence and exit angle of the incident and diffracted X-ray beam, respectively, with respect to the surface. Figure 9b shows the model obtained from GIXRD. Figure 9c shows an in-plane reciprocal space map for nearly zero Qz (perpendicular momentum transfer) from sample **1Si-1.** Qx, Qy and Qz directions have been chosen using the Si substrate lattice. Hence, Qx and Qy correspond to the parallel momentum transfer lying on the substrate surface along the Silicon a and b-axis, respectively. Qz corresponds to the perpendicular momentum transfer along the Silicon c-axis. A linear scan along Qx for Qy = 0 that includes Si (200) reflection is overlapped to the in-plane GIXRD data. The main feature in Figure 9c is the (040) diffraction peak (d = 4.147 Å) appearing at Q= 1.515 $Å^{-1}$ that can be assigned to an ordered network with the layer's a-axis perpendicular to the surface, like in Figure 9a. This network aligns one of its crystallographic axis to the Si substrate axis. As the b (green line in Figure 9a and 9b) and c (blue line in Figure 9a and 9b) lattice parameters from the layer of **2** are very similar, probably two in-plane domains are present (layer b-axis parallel to Si a-axis and layer c-axis parallel to Si a-axis, shown in yellow in Figure 9b). Although the peak shows tails at constant value of momentum transfer Q, indicating some mosaicity, the diffraction pattern evidences the formation of a highly oriented layer.

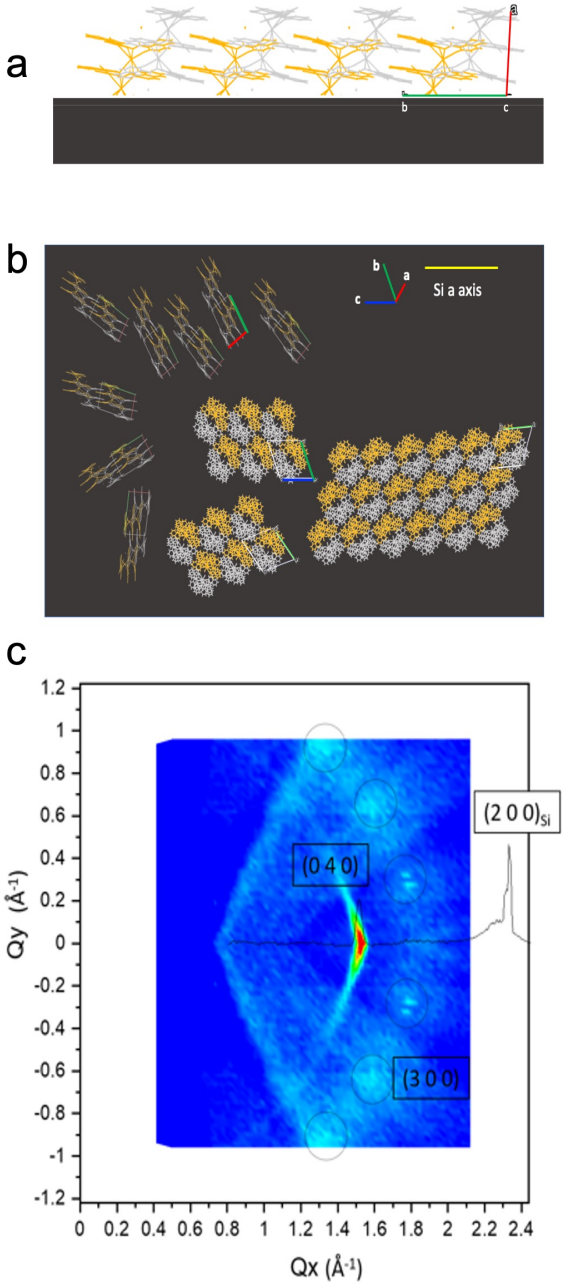

Figure 9. (a) Simple model for **1Si-1**, the supramolecular dimers are formed by molecules in grey and orange. (b) Model for **1Si-1** derived from GIXRD data. The unit cell axes of **1** are shown in red (a-axis), green (b-axis) and blue (c-axis). The model shows different domains with different orientations of the bc plane with respect to the Si a-axis (yellow line) and one domain with the c-axis perpendicular to the Si substrate. (c) GIXRD in-plane data for **1Si-1.**

At larger Q values, (300) diffraction peak (d = 3.39 Å) appearing at Q = 1.85 $Å^{-1}$ from a minority network with c-axis oriented out-of-plane is also observed. This network displays several in-plane domains rotated with respect to each other, resulting in several peaks. The model constructed from the GIXRD data, shown in Figure 9b, shows order of the molecules on the surface of the **Si-TSP** wafer, with a limited number of domains with the molecules in the same orientation. The sideways positioning of the molecules, with the c-axis perpendicular to the substrate is similar to the results obtained for simple phthalocyanine complexes on metallic surfaces.[3]

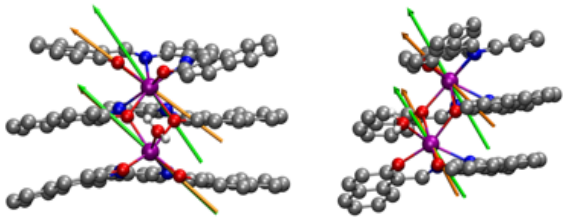

Figure 10. Two orientations of complex **2**, showing the Easy Axes of Magnetization (EAM) for each Dy in the ground state obtained with *ab initio* calculations (green arrows) and computed with Magellan (orange arrows).

Magnetic properties of **2** were previously reported by us,[13] this complex is a poor SMM with a blocking temperature below liquid helium. Complex **1** presents typical behavior for a Eu(III) dinuclear complex, with a χT value at 300 K of 2.7 cm^3 K /mol as expected for two Eu(III) ions (see ESI Figure S8). *Ab initio* theoretical calculations were performed on the $[Ln(SYML)_3(H_2O)]$ complexes. The electronic structure of the complex in compounds **1** and **2** have been explored with CASSCF calculations, see ESI for computational details. Both Eu ions in complex **1** show J=0 ground state (L=3, S=3) and are thus diamagnetic, as stated from the χT measures.

In contrast, both Dy atoms in compound **2** are found to display relatively low anisotropies. The computed ground state g-tensor for the octacoordinated Dy ion (Dy1) shows g_x = 0.383, g_y = 2.486, and g_z = 17.036, whereas the heptacoordinated Dy center (Dy2) has g_x = 0.607, g_y = 5.482, and g_z = 14.676. In this case the computed EAM for the Dy(III) atoms appear to be more collinear than those found for compound **1** (Figure 10). The estimated dipolar contribution to the magnetic coupling from the *ab initio* calculations amounts 1.1 K.

The relative orientation of the main anisotropy axis on the Dy ions can be also estimated with the software Magellan,[30] where a simple point charge model is employed. The results obtained with Magellan are similar to those obtained with the *ab initio* calculations; the main axes obtained for the octacoordinated Dy differ by 19º, while the axis for the heptacoordinated Dy is practically identical (5º).

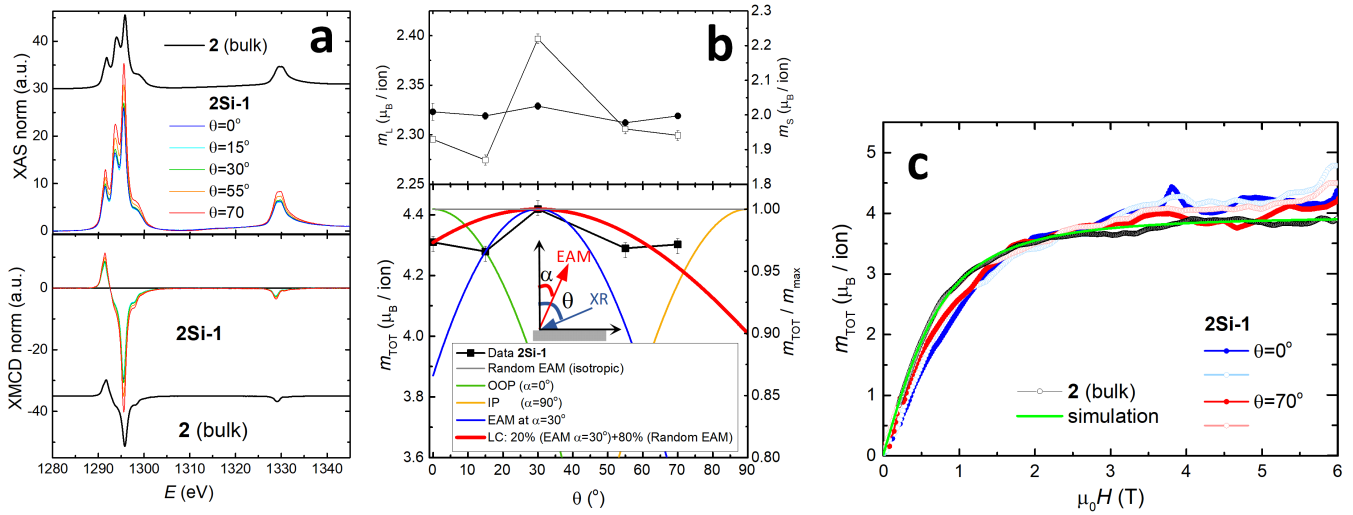

Figure 11. (a) XAS and XMCD spectra measured at 6 T and 4 K as a function of the beam incidence angle with respect to the normal (θ) for sample **2Si-1**, and at θ = 0º for powdered sample **2** (spectra have been shifted vertically for the sake of comparison); (b) field-dependence of the orbital (m_L), spin (m_S) and total magnetic moment (m_{TOT}). The bottom panel shows the predicted $m_{TOT}(\theta)$, normalized to the maximum value m_{max}, for molecules with their EAM oriented out-of-plane (OOP, α = 0º), in-plane (IP, α = 90º) and at an angle α = 30º ,with respect to the substrate-normal (see inset) and $m_{TOT}/m_{max}(\theta)$ simulation for the linear combination (LC) of a 20% of molecules with EAM oriented at α = 30º and a 80% fraction of molecules with randomly oriented EAM; (c) field-dependence of $m_{TOT}(H)$, for **2** and **2Si-1** (θ = 0º and θ = 70 º beam incidence) and theoretical prediction (green line) under a model of two interacting S* = 1/2 spins with the *ab initio* g values and J/k_B = 2.4 K at T = 4 K.

The *ab initio* EAM on the Dy ions in **2**, assuming a coordination to the carboxylato groups of TSP on the Si surface as that depicted in Figure 3b, would be at 63° (62° for the Magellan EAM) for Dy2 and 60° (64° for Magellan EAM) for Dy1 from the flat substrate. Apart from providing a robust anchoring on the surface, the coordination bond between the complex fragment and the surface could affect the axial magnetic anisotropy of the Dy-based compound.[31,32]

To investigate the magnetic properties of the grafted molecules, we measured the XAS and XMCD spectra at the Dy $M_{4,5}$ edge of **2Si-1** at 6 T and nominal temperature 1.6 K. The magnetic anisotropy was investigated by measuring the spectra as a function of the beam incidence angle with respect to the substrate normal (θ). Measurements for the bulk sample **2** at normal incidence $\theta = 0°$ were also performed for comparison (Figure 11a). The recorded XAS and XMCD for **2Si-1** and **2** show similar structure, coinciding with that expected for Dy^{3+} ions.[33] The orbital moment (m_L), spin moment (m_s) and total moment ($m_{TOT} = m_L + m_s$) per ion were determined from the XAS and XMCD spectra using the corrected sum rules for Dy^{3+} ion.[34,35] The correction is required to account for the large jj mixing between the $3d^{5/2}$ and $3d^{3/2}$ core levels, on the one hand, and the contribution of the $<T_z>$ magnetic dipole term, on the other. For **2** sum rules yielded m_L = 2.09 μ_B/ion, m_S = 1.89μ_B/ion and m_{TOT} = 3.88 μ_B/ion at 6 T.

Figure 11b summarizes the angular dependence of m_L, m_S, m_{TOT} (θ) obtained for **2Si-1**. The total magnetic moment reaches a maximum, m_{TOT} = 4.42 μ_B/ion at θ = 30°. However, the measured anisotropy is smaller than that expected for a system of molecules with EAM oriented at α = 30° with respect to the substrate normal (i.e *circa*. 60° from the substrate plane), as suggested by *ab initio* calculations and the model proposed from GIXRD. This is shown in Fig. 11(bottom), where we compare the angular dependence of the magnetic moment normalized to its maximum, $m_{TOT}(\theta)/m_{max}$, determined experimentally (black symbols) with the theoretical prediction for a system of molecules with their EAM oriented at an angle α=30° respect to the substrate normal (blue line). The Inset clarifies the geometrical configuration and the definition of angles. Figure 11(bottom) shows as well, for comparison, the predicted $m_{TOT}(\theta)/m_{max}$, dependence for system of molecules with their EAM oriented out-of-plane (OOP, α=0°, green line), EAM in-plane (IP, α=9°, yellow line), and the $m_{TOT}(\theta)/m_{max}$=1 constant (grey line) corresponding to an isotropic system of molecules with their EAM at random.

The small anisotropy observed indicates that only a fraction of the **2Si-1** molecules are efficiently grafted and have their EAM oriented at around α = 30°, whereas the rest lay on the surface with their EAM at random orientations. Indeed, the experimental $m_{TOT}/m_{max}(\theta)$ data can be rationalized considering a linear combination (LC) of 10%-20% of grafted molecules with their EAM at α= 30° and a 90%-80% of molecules with random EAM orientation (Figure 11b, red line).

Figure 11c shows the magnetic field dependence of the magnetic moment, $m_{TOT}(H)$, measured between 0 and 6 T for **2Si-1** in normal and grazing incidence. For the sake of comparison, the $m_{TOT}(H)$ cycle determined from XMCD at the same temperature and $\theta = 0°$ for the bulk (**2**) is shown too. The powder data can be fitted using a model of two interacting spins with effective spin S* = 1/2, with the gyromagnetic values predicted by *ab initio* for Dy1 and Dy2, and a ferromagnetic coupling of J/k_B = 2.4 K. From the fit it was found that the real temperature in the sample was 4 K, slightly above the set temperature of 1.6 K. The predicted m_{TOT} = 3.89 μ_B/ion is in very good agreement with the value obtained from sum rules at 6 T. Since the intramolecular dipolar coupling was calculated to be J_{dip}/k_B = 1.1 K, the exchange Dy-Dy coupling is found to be J_{ex}/k_B = 1.4 K. Complex **2** did not show hysteresis of the magnetization at 2 K.[13] For sample **2Si-1** the $m_{TOT}(H)$ cycles do not show hysteresis, as expected at 4 K. There is little difference between the curves measured in normal ($\theta = 0°$) and grazing ($\theta = 70°$) beam incidence, in agreement with the above described $m_{TOT}(\theta)$ dependence. However, the curvature of the $m_{TOT}(H)$ cycles is somewhat smoother than that of the powdered sample **2** measured in the same conditions, which may be plausibly ascribed to the contribution of the oriented molecules. In this sense, the molecules in **2Si-1** are in a monolayer of 1 nm, thus the dipolar interactions are markedly different that those found in the bulk sample **2**.

Conclusions

The use of TSP leads to a surface functionalized Si(100) wafers with carboxylato groups that can be used to graft SMMs or other magnetic molecules to a substrate following a mild, simple and reproducible protocol. Complexes **1** and **2** have been grafted on **Si-TSP** and the resulting samples **1Si** and **2Si** have been thoroughly characterized by ellipsometry, contact angle, AFM, XPS, emission spectra, ToF-SIMs and HAXPES. All these data show that we have achieved large area coverage of the **Si-TSP** wafer with both **1** and **2**. We successfully show how lanthanoid emission spectra can be used to track surface functionalization in a simple and straight-forward manner for the Eu complex **1Si**. The orientation of the molecules on the surface has been examined by GIXRD for **1Si**. The GIXRD data show ordered domains of the molecules on the surface. A model is drawn from these data that is tested with XMCD. Angle-dependent XAS and XMCD served to probe the magnetic

properties and anisotropy of Dy(III) in the molecular layer of **2Si**. The results corroborate a 10-20% of molecules following an ordered pattern as that in the model proposed from GIXRD data. The combination of GIXRD and XMCD is crucial to address large areas functionalized with molecules. Our results show that even if there is ample room for improvement in the 2D organization of molecules, the method proposed here can be used to achieve the two proposed goals: large area coverage and homogenous disposition of the molecules on the surface. Furthermore, the method can be easily adapted to on-surface chemistry or deposition of other complex molecules.

Conflicts of interest

There are no conflicts to declare.

Acknowledgements

ECS and GGR acknowledge financial support from the Spanish Government Ministerio de Ciencia Innovación y Universidades (project PGC2018-098630-B-I00 and PhD fellowship FPI PRE2019-087801 to GGR). JRZ acknowledges financial support from CSIC and Ministerio de Ciencia, Innovación y Universidades (projects 201060E013 and 202160E030). JJ acknowledges financial support from the Spanish Government Ministerio de Ciencia Innovación y Universidades (PGC2018-093863-B-C21 and MDM-2017-0767). EB acknowledge financial support from the Gobierno de Aragón (project RASMIA E12-20R). ECS, GG, EB acknowledge beamtime use at ALBA BOREAS (project 2021075217) and ESRF SpLine (project 25-02-964). The XAS/XMCD experiments were performed at BOREAS beamline at ALBA Synchrotron with the collaboration of ALBA staff.

Notes and references

1 E. Coronado, Molecular magnetism : from chemical design to spin control in molecules, materials and devices, *Nat. Rev. Mater.*, 2020, **5**, 87–104.
2 D. Gatteschi, A. Cornia, M. Mannini and R. Sessoli, Organizing and addressing magnetic molecules, *Inorg. Chem.*, 2009, **48**, 3408–3419.
3 K. Eguchi, Y. Takagi, T. Nakagawa and T. Yokoyama, Molecular orientation and electronic states of vanadyl phthalocyanine on Si(111) and Ag(111) surfaces, *J. Phys. Chem. C*, 2013, **117**, 22843–22851.
4 R. Bagai and G. Christou, The drosophila of single-molecule magnetism: [Mn12O12(O2CR)16(H2O)4], *Chem. Soc. Rev.*, 2009, **38**, 1011–1026.
5 M. Clemente-leo, E. Coronado, C. Mingotaud and P. Delhae, Langmuir ± Blodgett Films of Single-Molecule, *Angew. Chem. Int. Ed*, 1998, **37**, 2842–2845.
6 J. Gómez-Segura, J. Veciana and D. Ruiz-Molina, Advances on the nanostructuration of magnetic molecules on surfaces: The case of single-molecule magnets (SMM), *Chem. Commun.*, 2007, 3699–3707.
7 N. Domingo, E. Bellido and D. Ruiz-Molina, Advances on structuring, integration and magnetic characterization of molecular nanomagnets on surfaces and devices, *Chem. Soc. Rev.*, 2012, **41**, 258–302.
8 R. J. Holmberg and M. Murugesu, Adhering magnetic molecules to surfaces, *J. Mater. Chem. C*, 2015, **3**, 11986–11998.
9 A. Cornia, M. Mannini, R. Sessoli and D. Gatteschi, Propeller-Shaped Fe4 and Fe3M Molecular Nanomagnets: A Journey from Crystals to Addressable Single Molecules, *Eur. J. Inorg. Chem.*, 2019, **2019**, 552–568.
10 M. Mannini, F. Pineider, P. Sainctavit, C. Danieli, E. Otero, C. Sciancalepore, A. M. Talarico, M. A. Arrio, A. Cornia, D. Gatteschi and R. Sessoli, Magnetic memory of a single-molecule quantum magnet wired to a gold surface, *Nat. Mater.*, 2009, **8**, 194–197.
11 C. Wäckerlin, F. Donati, A. Singha, R. Baltic, S. Rusponi, K. Diller, F. Patthey, M. Pivetta, Y. Lan, S. Klyatskaya, M. Ruben, H. Brune and J. Dreiser, Giant Hysteresis of Single-Molecule Magnets Adsorbed on a Nonmagnetic Insulator, *Adv. Mater.*, 2016, **28**, 5195–5199.
12 L. Rosado Piquer, E. Jiménez Romero, Y. Lan, W. Wernsdorfer, G. Aromí and E. C. Sañudo, Hybrid molecular-inorganic materials: A heterometallic [Ni4Tb] complex grafted on superparamagnetic iron oxide nanoparticles, *Inorg. Chem. Front.*, 2017, **4**, 595–603.
13 L. R. Piquer, R. R. Sánchez, E. C. Sañudo and J. Echeverría, Understanding the molecule-electrode interface for molecular spintronic devices: A computational and experimental study, *Molecules*, 2018, **23**, 1441.
14 L. Rosado Piquer, M. Escoda-Torroella, M. Ledezma Gairaud, S. Carneros, N. Daffé, M. Studniarek, J. Dreiser, W. Wernsdorfer and E. Carolina Sañudo, Hysteresis enhancement on a hybrid Dy(iii) single molecule magnet/iron oxide nanoparticle system, *Inorg. Chem. Front.*, 2019, **6**, 705–714.
15 Y. Prado, N. Daffé, A. Michel, T. Georgelin, N. Yaacoub, J. M. Grenèche, F. Choueikani, E. Otero, P. Ohresser, M. A. Arrio, C. Cartier-Dit-Moulin, P. Sainctavit, B. Fleury, V. Dupuis, L. Lisnard and J. Fresnais, Enhancing the magnetic anisotropy of maghemite nanoparticles via the surface coordination of molecular complexes, *Nat. Commun.*, 2015, **6**, 10139.
16 C. A. P. Goodwin, F. Ortu, D. Reta, N. F. Chilton and D. P. Mills, Molecular magnetic hysteresis at 60 kelvin in dysprosocenium, *Nature*, 2017, **548**, 439–442.
17 C. A. Gould, K. R. Mcclain, D. Reta, J. G. C. Kragskow, D. A. Marchiori, E. Lachman, E. Choi, J. G. Analytis, R. D. Britt, N. F. Chilton, B. G. Harvey, J. R. Long, U. S. Navy, N. Air, N. Sciences, O. Rd, M. S. Division, L. Berkeley, N. High and M. Field, Ultrahard magnetism from mixed-valence dilanthanide complexes with metal – metal bonding, *Science (80-.).*, 2022, **375**, 198–202.
18 F. S. Guo, B. M. Day, Y. C. Chen, M. L. Tong, A. Mansikkamäki and R. A. Layfield, A Dysprosium Metallocene Single-Molecule Magnet Functioning at the Axial Limit, *Angew. Chemie - Int. Ed.*, 2017, **56**, 11445–11449.
19 F. S. Guo, B. M. Day, Y. C. Chen, M. L. Tong, A. Mansikkamäki and R. A. Layfield, Magnetic hysteresis up to 80 kelvin in a dysprosium metallocene single-molecule magnet, *Science (80-.).*, 2018, **362**, 1400–1403.
20 S. Gholizadeh Dogaheh, H. Khanmohammadi and E. C. Sañudo, Double-decker luminescent ytterbium and erbium SMMs with symmetric and asymmetric Schiff base ligands, *New J. Chem.*, 2017, **41**, 10101–10111.
21 M. Godoy-Gallardo, M. C. Manzanares-Céspedes, P. Sevilla, J. Nart, N. Manzanares, J. M. Manero, F. J. Gil, S. K. Boyd and D. Rodríguez, Evaluation of bone loss in antibacterial coated dental

implants: An experimental study in dogs, *Mater. Sci. Eng. C*, 2016, **69**, 538–545.
22 A. F. Stalder, G. Kulik, D. Sage, L. Barbieri and P. Hoffmann, A snake-based approach to accurate determination of both contact points and contact angles, *Colloids Surfaces A Physicochem. Eng. Asp.*, 2006, **286**, 92–103.
23 J. R. Rubio-Zuazo and G. R. Castro, Hard X-ray photoelectron spectroscopy (HAXPES) (≤15 keV) at SpLine, the Spanish CRG beamline at the ESRF, *Nucl. Instruments Methods Phys. Res. Sect. A Accel. Spectrometers, Detect. Assoc. Equip.*, 2005, **547**, 64–72.
24 J. Rubio-Zuazo, M. Escher, M. Merkel and G. R. Castro, High Voltage-Cylinder Sector Analyzer 300/15: A cylindrical sector analyzer for electron kinetic energies up to 15 keV, *Rev. Sci. Instrum.*, , DOI:10.1063/1.3398441.
25 S. Gholizadeh Dogaheh, J. Soleimannejad and E. C. Sanudo, Asymmetric Schiff base ligand enables synthesis of fluorescent and near-IR emitting lanthanide compounds, *J. Mol. Struct.*, 2020, **1219**, 129060.
26 Q. Li, P. Yan, P. Chen, G. Hou and G. Li, Salen Type Sandwich Triple-Decker Tri- and Di-nuclear Lanthanide Complexes, *J. Inorg. Organomet. Polym. Mater.*, 2012, **22**, 1174–1181.
27 R. Kunert, C. Philouze, O. Jarjayes and F. Thomas, *Inorg. Chem.*, 2019, 58, 8030–8044.
28 C. Caspers, M. Müller, A. X. Gray, A. M. Kaiser, A. Gloskovskii, C. S. Fadley, W. Drube and C. M. Schneider, Chemical stability of the magnetic oxide EuO directly on silicon observed by hard x-ray photoemission spectroscopy, *Phys. Rev. B - Condens. Matter Mater. Phys.*, 2011, **84**, 1–7.
29 E. E. Hardy, K. M. Wyss, R. J. Keller, J. D. Gorden and A. E. V. Gorden, Tunable ligand emission of napthylsalophen triple-decker dinuclear lanthanide(III) sandwich complexes, *Dalt. Trans.*, 2018, **47**, 1337–1346.
30 N. F. Chilton, D. Collison, E. J. L. McInnes, R. E. P. Winpenny and A. Soncini, An electrostatic model for the determination of magnetic anisotropy in dysprosium complexes, *Nat. Commun.*, , DOI:10.1038/ncomms3551.
31 L. Ungur and L. F. Chibotaru, Magnetic anisotropy in the excited states of low symmetry lanthanide complexes, *Phys. Chem. Chem. Phys.*, 2011, **13**, 20086–20090.
32 M. D. Korzyński, Z. J. Berkson, B. Le Guennic, O. Cador and C. Copéret, Leveraging Surface Siloxide Electronics to Enhance the Relaxation Properties of a Single-Molecule Magnet, *J. Am. Chem. Soc.*, 2021, **143**, 5438–5444.
33 S. O. Parreiras, D. Moreno, B. Cirera, M. A. Valbuena, J. I. Urgel, M. Paradinas, M. Panighel, F. Ajejas, M. A. Niño, J. M. Gallego, M. Valvidares, P. Gargiani, W. Kuch, J. I. Martínez, A. Mugarza, J. Camarero, R. Miranda, P. Perna and D. Écija, Tuning the Magnetic Anisotropy of Lanthanides on a Metal Substrate by Metal–Organic Coordination, *Small*, 2021, **17**, 2102753.
34 B. T. Thole and G. van der Laan, Sum rules for magnetic dichroism in rare earth 4f photoemission, *Phys. Rev. Lett.*, 1993, **70**, 2499–2502.
35 B. T. Thole, P. Carra, F. Sette and G. van der Laan, X-ray circular dichroism as a probe of orbital magnetization, *Phys. Rev. Lett.*, 1992, **68**, 1943–1946.